Diagn Interv Radiol 2022; DOI: 10.5152/dir.2022.201091

CHEST IMAGING

ORIGINAL ARTICLE

Dual-energy computed tomography iodine uptake in differential diagnosis of inflammatory and malignant pulmonary nodules

Lin Qiu*
Xue-Hui Pu*
Hai Xu
Tong-Fu Yu
Mei Yuan

PURPOSE
The aim of this study was to evaluate the diagnostic performance of iodine uptake parameters using dual-energy computed tomography (DECT) in discriminating inflammatory nodules from malignant tumors.

METHODS
This retrospective study included 116 solid pulmonary nodules from 112 patients who were admitted to our hospital between January and September 2018. All nodules were confirmed by surgery or puncture. The degree of enhancement of a single-section region of interest was evaluated. After total tumor volume-of-interest segmentation, the mean iodine density of the whole tumor was measured. Meanwhile, iodine uptake parameters, including total iodine uptake volume, total iodine concentration, vital iodine uptake volume, and vital iodine concentration, were calculated, and a predictive model was established. The overall ability to discriminate between inflammatory and malignant nodules was analyzed using an independent samples t-test for normally distributed variables. The diagnostic accuracy and prognostic performance of DECT parameters were evaluated and compared using receiver operating characteristic curve analysis and logistic regression analysis. A multivariate logistic regression analysis was used to determine the prognostic factors and goodness-of-fit of the whole tumor mean iodine and iodine uptake parameters for discriminating malignant nodules.

RESULTS
There were 116 non-calcified nodules, including 64 inflammatory nodules and 52 malignant nodules. The degree of enhancement in malignant nodules was significantly lower than that in inflammatory nodules ($P = .043$). All iodine uptake parameters in malignant nodules were significantly higher than those in inflammatory nodules ($P < .001$). The area under the receiver operating curve value, accuracy, sensitivity, and specificity of the established model based on iodine uptake parameters were 0.803, 76.72%, 82.69%, and 84.37%, respectively, which exhibited better diagnostic performance than the degree of enhancement on weighted average images with respective values of 0.609, 59.48%, 61.54%, and 59.38%.

CONCLUSION
The iodine uptake parameters of DECT exhibited better diagnostic accuracy in discriminating inflammatory nodules from malignant nodules than the degree of enhancement on weighted average images.

From the Department of Radiology (L.Q., X.-H.P., H.X., T.-F.Y., ✉ yu.tongfu@163.com), M.Y., ✉ yuanmeijiangsu@163.com, The First Affiliated Hospital of Nanjing Medical University, Nanjing, China.

* Dr. Lin Qiu and Xue-Hui Pu contributed equally to this work.

Received 11 January 2021; revision requested 18 February 2021; last revision received 7 August 2021; accepted 8 December 2021.

Publication date: 1 December 2022.

DOI: 10.5152/dir.2022.201091

Lung cancer is recognized as the most common and lethal type of malignancy worldwide, and its incidence is still on the rise.[1,2] Determining the likelihood of malignancy in solitary pulmonary nodules (SPNs) is important for treatment selection and prognosis evaluation.

Conventional thoracic contrast-enhanced computed tomography (CT) has been the major method used for examining pulmonary nodules. Malignant nodules are usually large, irregular in shape, and lack smooth edges, in contrast to benign nodules. In addition, the degree of enhancement of malignant nodules is positively correlated with the expression level of vascular endothelial growth factor and microvessel density. Thus, malignant nodules often show a higher degree of enhancement than benign nodules.[3] However, some types of lung inflammation, such as granuloma or organizing pneumonia, show morphological features

You may cite this article as: Qiu L, Pu X, Xu H, Yu T, Yuan M. Dual-energy computed tomography iodine uptake in differential diagnosis of inflammatory and malignant pulmonary nodules. *Diagn Interv Radiol.* 2022;28(6):563-568.

similar to malignant nodules on CT images, and the rich, dilated capillaries are stimulated by inflammation, making them difficult to distinguish from malignant nodules. Ohno et al.[4] summarized previous research on the value of dynamic contrast-enhanced CT for pulmonary nodule assessment. They found that the specificity of contrast-enhanced CT in discriminating benign and malignant nodules varied from 52% to 93%. Moreover, the measurement of CT values can be easily affected by water, air, and calcification. The tumor itself, matrix, and contrast agent also have an impact on CT measurements.[5]

Recently, dual-energy CT (DECT) has rapidly gained popularity for clinical practice, which can improve material differentiation by using two different x-ray effective energies. Current DECT acquisition methods consist of dual tubes either with or without beam filtration, rapid voltage switching with a single tube, a dual-layer detector with a single tube, a single tube with a split filter, or a single tube with sequential dual scans. Dual-source DECT features a 3-substance (fat, soft tissue, and iodine) separation algorithm, which can eliminate the influences of calcification and necrosis on the evaluation of nodules. Moreover, DECT can accurately separate and quantify iodine in each pixel of the enhanced image. An iodine map can be subsequently isolated from the mixed images and can provide information about the distribution of iodinated contrast media in the target organ. As a result, it directly reflects the degree of enhancement at the lesion and provides information about the blood supply of the tumor, which can be more accurate in evaluating the nature of the pulmonary nodules.[6]

A series of studies[7-9] have demonstrated the significance of DECT iodine uptake parameters in the evaluation of malignancy, curative effect, and prognosis in the lungs (and other organs). It was shown that DECT-based iodine content measurement could separate benign from malignant tumors, with 93.8% sensitivity and 85.7% specificity in pulmonary nodules[9] and 97% sensitivity and 100% specificity in differentiating adrenal adenoma from metastases.[9] Moreover, iodine uptake parameters may help evaluate treatment response in non-small cell lung cancer.[10] Lin et al.[11] evaluated the iodine uptake parameters of benign and malignant SPNs. The iodine uptake parameters of malignant SPNs were significantly lower than those of inflammatory SPNs, on the contrary, significantly higher than those of tuberculoma. Few studies have evaluated the value of iodine uptake parameters for differentiating inflammatory nodules independently. The purpose of our study was to investigate the clinical utility of iodine uptake parameters using DECT for discriminating pulmonary inflammatory nodules from malignant nodules.

Main points

- The degree of enhancement based on single-section region of interest (ROI) was significantly higher in inflammatory nodules than that in malignant nodules. However, the mean iodine and iodine uptake parameters of dual-energy computed tomography (DECT) based on whole tumor were totally different.
- A model established with the iodine uptake parameters provides an accurate method to discriminate inflammatory nodules from malignant nodules, which was more accurate and specific than the degree of enhancement on single-section ROI.

Methods

Patients

Ethical approval was obtained from our institutional review board (2018-SRFA-139), due to the retrospective nature of the study informed consent need was waived. We systematically reviewed 462 patients who underwent thoracic DECT at our institution between January and September 2018. Patients meeting the following criteria were enrolled in our study: (a) all lesions manifested as solid nodules ≤3.0 cm in the greatest dimension without calcification; (b) patients received antibiotic therapies for at least 2 weeks before the DECT scan, and lesions showed no or slight changes (<20% total increase in size according to revised Response Evaluation Criteria In Solid Tumours (RECIST) guideline version 1.1), which were difficult to diagnose clinically; (c) preoperative non-enhanced thin-section CT and DECT scans were performed simultaneously; (d) pathological results were determined by CT-guided percutaneous biopsy or surgical resection within 6 weeks after DECT; (e) patients had no radiation therapy or chemotherapy before surgery.

A total of 350 patients were excluded based on at least one of the following criteria: (a) no simultaneous non-enhanced CT scan (n = 163); (b) unsatisfactory imaging quality due to respiratory artifacts during the examination (n = 32); (c) CT-guided percutaneous biopsy was performed before the CT scan (n = 45); (d) lesion size >3 cm (n = 35); (e) direct invasion of malignant nodules of the chest wall, phrenic nerve, parietal pericardium, diaphragm, mediastinum, heart, great vessels, trachea, recurrent laryngeal nerve, oesophagus, vertebral body, or carina (n = 28); (f) distant or lymph node metastasis (n = 32); (g) thin-walled cystic lesions (n = 5) or nodules with extensive cavities (n = 10).

CT scanning

All patients underwent preoperative non-enhanced and contrast-enhanced thin-section CT examinations using third-generation dual-source CT (Somatom Force; Siemens Healthcare).

Non-enhanced CT scans were performed using single-energy CT with tin filtration (collimation, 192 × 0.6 mm; pitch, 1.2; rotation time, 0.5 s). The tube voltage was set at 100 Sn kVp with CareDose4D mAs, and spectral shaping was 1/10th the dose. Advanced model-based iterative reconstruction (ADMIRE)-strengthened level 3 was used for the iterative reconstruction.

All patients underwent contrast-enhanced CT in the craniocaudal direction with elevated arms using a dual-energy protocol (collimation, 192 × 0.6 mm; pitch, 0.55; rotation time, 0.25 s). The tube voltages were set at 90 kVp and 150 Sn kVp using a 0.6-mm tin filter. The reference tube current–time products were 1.3 : 1 for 90 kVp and 150 kVp (tube A, 80 mAs; tube B, 62 mAs) with automated modulation. ADMIRE level 3 was used for iterative reconstruction. Three different sets of images were acquired from the DECT scan: 90 kVp, 150 Sn kVp, and weighted average image (the ratio from tube A and tube B was 0.6 : 0.4). The iodinated contrast agent (Ultravist, 370 mg I/mL) was injected intravenously using a dual-head power injector (Medrad Stellant) at a rate of 4 mL/s, amount of weight × 1.5 mL, followed by 30 mL of saline chaser at the same injection rate. Thin-section CT scans were obtained at 40 and 100 s after the onset of injection.

Imaging analysis

Dual-energy data sets were reconstructed using a section thickness of 1.0 mm and an increment of 0.8 mm with a standard mediastinal kernel (Q40). The single-section region of interest (ROI) was manually outlined on the DECT-weighted

average image of the venous phase at the section where the tumors appeared to be the largest for measuring the degree of enhancement. Visually identified vessels, cavities, and necrotic areas were excluded. The drawn ROIs were automatically transferred to non-enhanced CT images using in-house software. The data sets were then post-processed using a modified prototype of the Liver Virtual Non-contrast Imaging (VNC) application class on a dual-energy workstation (Syngo.via, version VA30A; Siemens Healthcare). Virtual non-enhanced and iodine-enhanced images were generated. Total tumor volume of interest (VOI) of each nodule from the weighted average image of DECT was automatically segmented by running on lungCAD software (Syngo.via; Siemens Healthcare) and manually adjusted to encompass the entire lesion in each image by two thoracic radiologists independently (author 1 and author 2 with 3 and 6 years of experience in thoracic imaging, respectively), and they were blinded to the patients' pathological diagnoses and clinical information. The segmented VOIs were transferred to non-enhanced CT images and in-house software by Siemens for measuring iodine uptake. The mean iodine density of the whole tumor and iodine uptake parameters including total iodine uptake, total iodine concentration (iodine concentration indicates the iodine uptake per unit volume), vital iodine uptake, and vital iodine concentration were calculated ("vital" means the remaining part of the tumor after removing the necrotic area of the tumor). The mean iodine density of the whole tumor and iodine uptake parameters of the inflammatory nodules and malignant nodules were calculated (Figure 1).

Statistical analysis

All statistical analyses were performed with the statistical packages SPSS version 20.0 and MedCalc version 8.2.0.1. A $P < .05$ was regarded as statistically significant. The normality and homoscedasticity of the image data were tested using Shapiro–Wilk tests and Levene's tests. Inter-observer reliability of 2 data sets independently measured by 2 radiologists was assessed by the inter-class correlation coefficient (ICC) introduced previously.[12] ICC values of 0.40-0.60, 0.61-0.80, and 0.81-1.00 indicate good, moderate, and excellent reproducibility, respectively.

Pearson chi-square test was used for comparison of qualitative data between groups. The overall ability to discriminate between inflammatory and malignant nodules was analyzed using an independent samples t-test for normally distributed variables. If a significant difference was obtained, the receiver operating characteristic (ROC) regression curve was quantified using the area under the ROC curves (AUC). The diagnostic accuracy, sensitivity, and specificity were calculated and compared at a cut-off point that maximized the value of the Youden index. A multivariate logistic regression analysis was used to determine the prognostic factors and goodness-of-fit of the mean iodine density of the whole tumor and iodine uptake parameters for discriminating malignant nodules.

Results

In total, 116 lesions in 112 patients were enrolled in the study (52 men with a mean age of 61.87 ± 9.28 years and 60 women with a mean age of 56.11 ± 12.94 years).

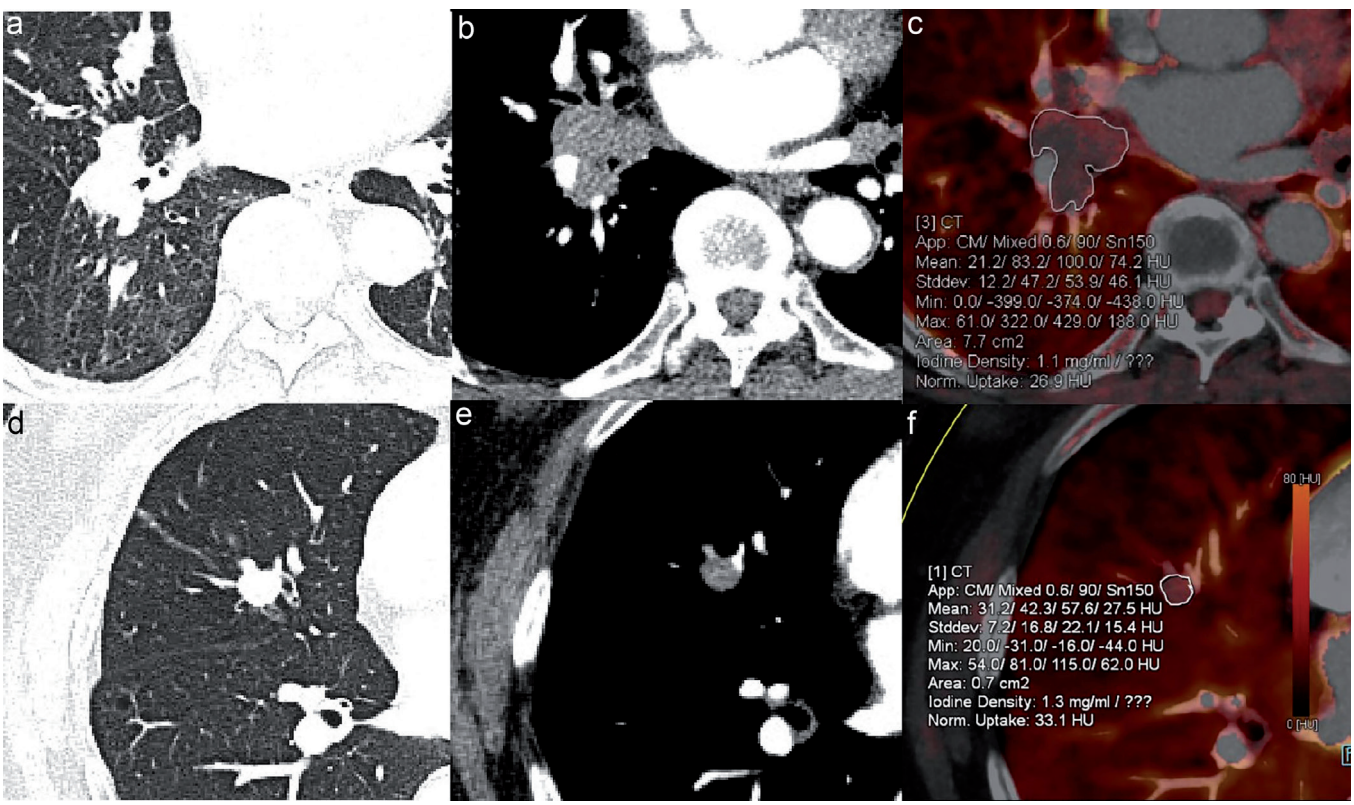

Figure 1. **(a)** A 72-year-old man with a lesion in the lower lobe of the right lung. Puncture result shows acute inflammatory cell infiltration. **(b)** Dual energy CT arterial phase shows the CT enhancement of the total nodule is 26.9 HU. **(c)** Iodine-enhanced image shows the vital iodine concentration is 1.1 mg/mL. **(d)** A 61-year-old man with adenocarcinoma in the middle lobe of the right lung. **(e)** Dual energy CT arterial phase shows the CT enhancement of the total nodule is 33.1 HU. **(f)** Iodine-enhanced image shows the vital iodine concentration is 1.3 mg/mL.

Table 1. Summary of clinical and pathologic characteristics of included nodules

Characteristics	Malignant nodules (n = 52)	Inflammatory nodules (n = 64)	*P*
Age (year)	61.98 ± 9.86	59.02 ± 12.54	.268[a]
Sex (male/female)	25 (48.1%)/27 (51.9%)	30 (46.9%)/34 (53.1%)	.897[b]
Smoking history (yes/no)	21 (40.4%)/31 (59.6%)	28 (43.8%)/36 (56.2%)	.715[b]
Lesion location			
Upper lobe	28 (53.8%)	30 (46.9%)	.748[b]
Middle lobe	8 (15.4%)	12 (18.8%)	
Lower lobe	16 (30.8%)	22 (34.3%)	
Maximum diameter (cm)	1.86 ± 0.45	1.81 ± 0.47	.507[a]

Values are presented as no. (%) or mean ± standard deviation.
[a]Student t-test. [b]Pearson chi-square test .

Among them, 62 patients were diagnosed with inflammatory nodules (64 nodules, 55.2%), and 50 patients had malignant nodules (52 nodules, 44.8%, which include 40 adenocarcinoma and 12 squamous cell carcinoma). The nodules are all well-defined, and the average maximum diameter of benign nodules is smaller than that of malignant nodules, and the density is more uniform. There were 56 lesions confirmed by surgery, and 60 lesions were confirmed by puncture. The details are presented in Table 1.

The inter-observer reliability was moderate to good for the parameters derived from the single-section ROI (range: 0.62-0.74) and excellent for whole-tumor volume placement (range: 0.85-0.95). Inter-observer agreement of whole-tumor analysis was better than that of single-section ROIs.

Malignant nodules showed a significantly lower degree of enhancement on single-section ROIs ($P = .043$) and significantly higher whole tumor mean iodine and iodine uptake than inflammatory nodules ($P < .001$). The details are presented in Table 2. The results of ROC analysis demonstrated that all 4 iodine uptake parameters showed significantly higher AUC values than the mean iodine density of the whole tumor (0.774-0.799 vs. 0.638). Total and vital iodine uptake volume showed higher sensitivity (both 80.77%) and total iodine concentration showed higher specificity (87.50%) than other iodine uptake parameters, without a statistically significant difference. The details are presented in Table 3.

A regression model of iodine uptake was generated by multivariate logistic regression analysis, and the Akaike information criterion (AIC) was used as a measure of goodness-of-fit. The accuracy of the iodine uptake model for differentiating malignant nodules from inflammatory nodules was 76.72% with ROC curve analysis (AUC, 0.803; sensitivity, 82.69%; specificity, 84.37%), which exhibited better diagnostic performance than mean iodine with an accuracy of 61.81% (AUC, 0.638; sensitivity, 67.31%; specificity, 57.81%). The iodine uptake model exhibited a better goodness-of-fit than mean iodine with AIC values of 63.8% and 45.3%, respectively, as illustrated in Table 4 and Figure 2.

Table 2. Comparison of multiple parameters between inflammatory and malignant nodules

Variables	Inflammatory nodules (n = 64)	Malignant nodules (n = 52)	*P*
Value of VNC (HU)	32.83 ± 1.96	29.16 ± 2.47	.241[a]
Degree of enhancement (HU)	34.37 ± 2.14	29.16 ± 2.47	.043[a]
Mean iodine (HU)	16.74 ± 1.94	31.12 ± 2.18	<.001[a]
Total iodine uptake (mg)	12.81 ± 5.83	31.38 ± 5.95	<.001[a]
Total iodine concentration (mg/mL)	0.62 ± 0.08	1.22 ± 0.09	<.001[a]
Vital iodine uptake (mg)	12.96 ± 5.92	32.03 ± 6.06	<.001[a]
Vital iodine concentration (mg/mL)	0.63 ± 0.08	1.28 ± 0.09	<.001[a]

Values are presented as mean ± standard deviation.
[a]$P < .05$ between inflammatory and malignant nodules with Mann–Whitney U test.

Discussion

Our study developed a new model based on iodine uptake parameters, including total iodine uptake, total iodine concentration, vital iodine uptake, and vital iodine concentration. The newly developed model exhibited better diagnostic performance and goodness-of-fit than the degree of mean iodine for discriminating inflammatory nodules from malignant nodules, with an accuracy of 76.72%, AUC of 0.803, sensitivity of 82.69%, specificity of 84.37%, and AIC of 63.8%.

In previous studies,[13,14] an enhancement value of 20 HU was mostly used as the critical value for distinguishing benign and malignant SPNs. A value greater than 20 HU suggests a malignant lesion or the lesion is benign. However, it is not possible to distinguish malignant nodules from benign nodules only by a difference in the net CT number. In previous studies, the specificity of contrast-enhanced CT in discriminating between benign and malignant nodules varied from 52% to 93%. Zhang et al.[8] found that without including the inflammatory nodules in 63 cases, the specificity and sensitivity for determining benign or malignant nodules based on the enhanced CT values were only 53.8% and 74.2%, respectively. The determination of the cut-off CT value is limited by many factors, including the size of the tumor, the type of benign nodules, and the impact of beam-hardening effects.[8]

As a type of benign nodule, inflammatory nodules have complex types, and the proportions of their blood vessel components change significantly as the disease progresses. In the early stages, inflammatory nodules consist primarily of vascular hyperplasia. Because the vascular density is high, the enhancement is generally significant in enhanced scans, and the degree of enhancement is even higher than that of lung cancer.[15] However, as the disease progresses, the new blood vessels in the nodules gradually occlude, the fibrous tissue proliferates, and the density of the blood vessels decreases. Therefore, the degree of enhancement may be decreased and may not be significantly enhanced. In summary, the enhancement patterns of inflammatory nodules vary at different stages of progression. In our study, all the benign nodules were inflammatory. The degree of enhancement based on a single-section ROI was higher than that of malignant nodules, which is consistent with the results of previous studies.[7,16] As the degree

Table 3. Effectiveness of the model based on iodine uptake parameters and the mean iodine on weighted average image in diagnosis of inflammatory nodules and malignant nodules

Factor	SEN (%)	SPE (%)	Accuracy (%)	Cut-off	Az
Degree of enhancement (HU)	61.5 (45.9–75.5)	59.4 (40.4–73.5)	59.5 (42.6–74.2)	≤28.6	0.609 (0.514–0.699)
Mean iodine (HU)	67.3 (48.2–85.6)	57.8 (37.9–73.1)	61.8 (46.7–79.4)	>25.53	0.638 (0.587–0.747)
Model	82.7 (67.4–91.0)	84.4 (64.9–95.2)	76.7 (60.1–88.7)	>0.41	0.803 (0.719–0.871)
Total iodine uptake (mg)	80.8 (64.6–90.0)	78.1 (63.4–88.9)	61.2 (45.4–74.9)	>2.24	0.798 (0.713–0.867)
Total iodine concentration (mg/mL)	65.4 (52.0–80.5)	87.5 (78.2–96.5)	76.7 (60.1–88.7)	>1.11	0.774 (0.687–0.847)
Vital iodine uptake (mg)	80.8 (64.6–90.0)	78.1 (63.4–88.9)	61.2 (45.4–74.9)	>2.24	0.799 (0.714–0.867)
Vital iodine concentration (mg/mL)	73.1 (52.2–88.4)	85.9 (65.1–95.5)	79.3 (63.6–89.1)	>1.11	0.789 (0.704–0.859)

SEN, sensitivity; SPE, specificity; Az, area under the receiver operating curve.

Table 4. Multivariable-based regression models for distinguishing inflammatory and malignant nodules

Parameter	Mean iodine (HU)	Iodine uptake model
Model-fitting information		
Akaike information criterion (%)	45.3	63.8
P	<.001	<.001
R^2 value	0.199	0.283

of enhancement of inflammatory nodules was slightly higher than that of malignant nodules (34.37 ± 2.14 vs. 29.16 ± 2.47, *P* = .043), using 20 HU as the cut-off value would not be suitable for our study. According to the ROC curve analysis, using 30 HU as the cut-off value in our study yielded the best predictive performance of the net CT number. The accuracy, specificity, and sensitivity were 59.48%, 59.38%, and 61.54%, respectively. The low specificity was consistent with previous results of predicting benign and malignant nodules.

Meanwhile, our study demonstrated that mean iodine values based on whole tumors were significantly lower in inflammatory nodules than in malignant nodules, in contrast to the degree of enhancement based on single-section ROI being lower in the malignant nodules. This finding has not been reported in previous studies. The potential reason may be that the measurement of the enhancement value can be easily affected by the ROI. Visually identified vessels, cavities, and necrotic areas were excluded from the single-section measurements. Moreover, because of tumor heterogeneity in the vital part of the tumor, the ROI on single-section slices showed intra-observer and inter-observer variability. Thus, a whole-tumor volume-based mean iodine enhancement approach may be a more promising way to determine enhancing patterns compared with single-section ROI measurement.

Sustained angiogenesis is one of the hallmarks of malignant tumors,[17] and new blood vessels offer higher iodine uptake. A series of studies[18,19] have confirmed a good correlation between iodine concentration and blood perfusion in tumors. In our study,

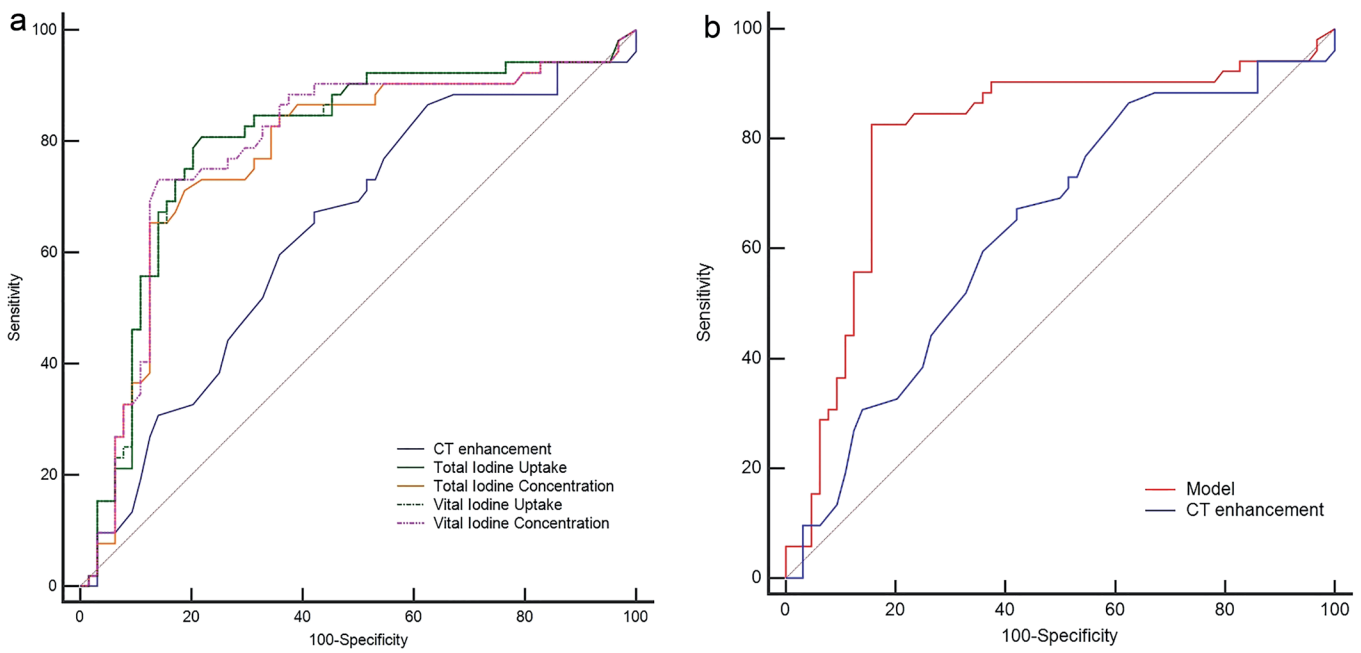

Figure 2. **(a)** ROC analysis of the 4 iodine uptake parameters for distinguishing inflammatory nodules from malignant nodules. **(b)** ROC analysis of the predictive model based on iodine uptake parameters and degree of enhancement on weighted average image image for distinguishing inflammatory nodules from malignant nodules. ROC, receiver operating characteristic curve.

the iodine uptake parameters, including total iodine uptake, total iodine concentration, vital iodine uptake, and vital iodine concentration, were significantly higher in malignant nodules than in inflammatory nodules, because the density of new blood vessels and vascular perfusion were higher, and the measures related to iodine uptake were correspondingly increased. DECT can be used to separate the substances to obtain an iodine map of the iodine contrast medium in the target organ. Quantifying the iodine content of the lesion, the map directly reflects the enhancement of the lesion and excludes the interference of water, air, and calcification. Moreover, with the mixed necrotic areas removed from the lesion, the iodine-related measures could more effectively reflect the perfusion inside the tumor. Ascenti et al.[20] in a study on renal tumors that were compared with the standard measurement of CT enhancement degree found that the iodine concentration of the entire lesion could more accurately distinguish the degree of iodine enhancement at the lesion. Other studies[21,22] have shown that in the evaluation of tumor treatment, CT values are not sufficiently sensitive for the early evaluation of targeted therapy owing to factors that increase tumor heterogeneity, such as internal necrosis and hemorrhage. The iodine concentration measured by DECT was superior to the CT values for the evaluation of the tumor blood supply. Previous studies[13] found that iodine-enhanced images showed higher sensitivity (92.0% vs. 72.0%), similar specificity (70.0% vs. 70.0%), and higher diagnostic accuracy (82.2% vs. 71.1%) compared with the degree of enhancement obtained by subtracting Hounsfield units from real non-enhanced images from Hounsfield units from real enhanced images. In our study, the model established with the iodine uptake parameters was more accurate and specific than the degree of enhancement on the weighted average image in differentiating the inflammatory and malignant nodules. This also reflected the superiority of the iodine uptake measures compared to the CT value, which is consistent with previous findings.[7]

There are some limitations to our study. First, external validation was absent because of the relatively small sample size. Second, our study focused only on the venous phase, as it reflects the quantity of vessels and blood flow, whereas the measurement in the venous phase was absent; therefore, further investigations are needed. Third, previous studies have counted the morphology-related characteristics of inflammatory and malignant nodules and used them to distinguish between the 2. For instance, necrosis and pleural thickening are more commonly observed in inflammatory nodules than in malignant nodules. These characteristics were not included in this study. It is believed that the combination of iodine uptake and morphological characteristics will provide more favorable diagnostic results.

In conclusion, the iodine uptake parameters of DECT provide a new method to discriminate inflammatory nodules from malignant nodules and exhibit better diagnostic accuracy in discriminating inflammatory nodules from malignant nodules than the degree of enhancement on weighted average images.

Conflict of interest disclosure

The authors declared no conflicts of interest.

References

1. Siegel R, Ma J, Zou Z, Jemal A. Cancer statistics, 2014. *CA Cancer J Clin*. 2014;64(1):9-29. [CrossRef]
2. Herbst RS, Heymach JV, Lippman SM. Lung cancer. *N Engl J Med*. 2008;359(13):1367-1380. [CrossRef]
3. Rosado de Christenson ML. Dynamic MRI of solitary pulmonary nodules: comparison of enhancement patterns of malignant and benign small peripheral lung lesions. *Year Book Diagn Rad*. 2008/01;2008:33-34. [CrossRef]
4. Ohno Y, Nishio M, Koyama H, et al. Dynamic contrast-enhanced CT and MRI for pulmonary nodule assessment. *AJR Am J Roentgenol*. 2014 03/01;202(3):515-529. [CrossRef]
5. Kawai T, Shibamoto Y, Hara M, Arakawa T, Nagai K, Ohashi K. Can dual-energy CT evaluate contrast enhancement of ground-glass attenuation? Phantom and preliminary clinical studies. *Acad Radiol*. 2011/01;18(6):682-689. [CrossRef]
6. Uhrig M, Sedlmair M, Schlemmer HP, Hassel JC, Ganten M. Monitoring targeted therapy using dual-energy CT: semi-automatic RECIST plus supplementary functional information by quantifying iodine uptake of melanoma metastases. *Cancer Imaging*. 2013;13(3):306-313. [CrossRef]
7. Hou W, Wu H, Yin Y, Cheng J, Zhang Q, Xu J. Differentiation of lung cancers From inflammatory masses with dual-energy spectral CT imaging. *Acad Rad*. 2014;12/06;22.
8. Zhang Y, Cheng J, Hua X, et al. Can spectral CT imaging improve the differentiation between malignant and benign solitary pulmonary nodules? *PLOS ONE*. 2016;11(2):e0147537. [CrossRef]
9. Martin S, Weidinger S, Czwikla R, et al. Iodine and fat quantification for differentiation of adrenal gland adenomas From metastases using third-generation dual-source dual-energy computed tomography. *Invest Rad*. 2017;53:1.
10. Fehrenbach U, Feldhaus F, Kahn J, et al. Tumour response in non-small-cell lung cancer patients treated with chemoradiotherapy - Can spectral CT predict recurrence? *J Med Imaging Radiat Oncol*. 2019;63(5):641-649. [CrossRef]
11. Lin JZ, Zhang L, Zhang CY, Yang L, Lou HN, Wang ZG. Application of gemstone spectral computed tomography imaging in the characterization of solitary pulmonary nodules: preliminary result. *J Comput Assist Tomogr*. 2016;40(6):907-911. [CrossRef]
12. Kang Y, Lee JW, Koh YH, et al. New MRI grading system for the cervical canal stenosis. *AJR Am J Roentgenol*. 2011;197(1):W134-W140. [CrossRef]
13. Chae EJ, Song JW, Krauss B, et al. Dual-energy computed tomography characterization of solitary pulmonary nodules. *J Thorac Imaging*. 2010;25(4):301-310. [CrossRef]
14. Lu GM, Zhao YE, Zhang LJ, Schoepf UJ. Dual-energy CT of the lung. *AJR Am J Roentgenol*. 2012;199(5):S40-S53. [CrossRef]
15. Yang ZG, Chen TW, Yu JQ, Sun JY, Chen HJ, Chen HJ. First-pass perfusion imaging of solitary pulmonary nodules with 64-detector row CT: comparison of perfusion parameters of malignant and benign lesions. *Br J Radiol*. 2010;83(993):785-790. [CrossRef]
16. Chu ZG, Sheng B, Liu MQ, Lv FJ, Li Q, Ouyang Y. Differential diagnosis of solitary pulmonary inflammatory lesions and peripheral lung cancers with contrast-enhanced computed tomography. *Clinics (Sao Paulo)*. 2016;71(10):555-561. [CrossRef]
17. Hanahan D, Weinberg RA. Hallmarks of cancer: the next generation. *Cell*. 2011;144(5):646-674. [CrossRef]
18. Zhang LJ, Wu S, Wang M, et al. Quantitative dual energy CT measurements in rabbit VX2 liver tumors: comparison to perfusion CT measurements and histopathological findings. *Eur J Radiol*. 2012;81(8):1766-1775. [CrossRef]
19. Klauss M, Stiller W, Pahn G, et al. Dual-energy perfusion-CT of pancreatic adenocarcinoma. *Eur J Radiol*. 2013;82(2):208-214.
20. Ascenti G, Mileto A, Krauss B, et al. Distinguishing enhancing from nonenhancing renal masses with dual-source dual-energy CT: iodine quantification versus standard enhancement measurements. *Eur Radiol*. 2013;23(8):2288-2295. [CrossRef]
21. Godoy MC, Naidich DP, Marchiori E, et al. Basic principles and postprocessing techniques of dual-energy CT: illustrated by selected congenital abnormalities of the thorax. *J Thorac Imaging*. 2009;24(2):152-159. [CrossRef]
22. Toepker M, Moritz T, Krauss B, et al. Virtual non-contrast in second-generation, dual-energy computed tomography: reliability of attenuation values. *Eur J Radiol*. 2012;81(3):e398-e405. [CrossRef]